Journal of Alloys and Compounds 491 (2010) 72–76

Contents lists available at ScienceDirect

Journal of Alloys and Compounds

journal homepage: www.elsevier.com/locate/jallcom

Ultra-low turn-on field from ultra-long ZnO nanowire arrays emitters

Gang Meng[a], Xiaodong Fang[a,b,*], Yikai Zhou[c], JongUk Seo[c], Weiwei Dong[a,b], Shigehiko Hasegawa[c], Hajime Asahi[c], Hiroyuki Tambo[c], Mingguang Kong[d], Liang Li[d]

[a] Anhui Institute of Optics and Fine Mechanics, Chinese Academy of Sciences, Hefei 230031, China
[b] Key Laboratory of New Thin Film Solar cells, Chinese Academy of Sciences, Hefei 230031, China
[c] The Institute of Scientific and Industrial Research, Osaka University, Osaka 5670047, Japan
[d] Key Laboratory of Materials Physics, Institute of Solid State Physics, Chinese Academy of Sciences, Hefei 230031, China

ARTICLE INFO

Article history:
Received 26 October 2009
Received in revised form 2 November 2009
Accepted 3 November 2009
Available online 13 November 2009

Keywords:
Field emission, ZnO nanowire arrays

ABSTRACT

Ultra-long and well-aligned ZnO nanowire arrays have been synthesized on p-Si (8–13 Ω cm) substrates by vapor phase transport (VPT) method. The length of the nanowire arrays can be modified by adjusting the distance between the source and substrates. Their field emission properties were investigated and the lowest turn-on voltage was observed at 1.08 V/μm. The exceptional field emission performances are attributed to the intrinsically high aspect ratios of ultra-long ZnO nanowire arrays. Our results show another feasible route to enhance field emission performance of ZnO nanowire arrays.

1. Introduction

Field emission (FE) has attracted great attention due to its numerous applications in flat panel display (FPD), electron microscope, electron spectroscopy, luminescent tube and other vacuum electronic devices that require electron sources [1–4]. Arrays of one-dimensional (1-D) nanostructures with high aspect ratio, proper areal density are suitable to produce high FE current at moderate electric field [5]. 1-D nanostructure arrays, such as carbon nanotubes (CNTs), ZnO, GaN, ZnS and AlN have been considered to be good cold cathode materials for FE applications [6–10]. Among these promising candidates, inherent n-type conductivity of 1-D ZnO nanostructures, their thermal stability and oxidation resistance justify them as potential cathode material for FE [5].

Following the first study of FE property of well-aligned ZnO nanowires by Lee et al. [11], much attention has been paid to investigate and improve the performances of 1-D ZnO field emitters, including lower turn-on field, higher FE current and higher stability, etc. Generally, two routes are widely adopted to improve the field emission performances. One route is to lower the work function of ZnO emitters by annealing in hydrogen ambience [12], hydrogen plasma treatment [13], through doping [14] or coupling with other materials [15,16]. The other route is to increase the aspect ratio (ratio of the length to tip radius) of emitters by fabrication nanopencils or nanoneedles with sharp emission tips [17–20]. Table 1 lists the key parameters of some 1-D ZnO field emitters in the previous literatures. It can be clearly seen that FE performances have been greatly enhanced by using above approaches [5,7–15]. Herein, we adopt another approach which is not to minimize the tip radius of emitter but to increase the length of ZnO nanowire arrays. We find a facile approach to fabricate ultra-long ZnO nanowire arrays with length varying via a one-step vapor phase transport (VPT) process, and the aspect ratio can be controlled gradually by adjusting the length of nanowires. FE characterization indicates the extremely low turn-on field voltages (the lowest one is about 1.08 V/μm) and high field enhancement factor were achieved.

2. Experimental procedure

Synthesis of vertically-aligned and ultra-long ZnO nanowire arrays was carried out in a tubular electric resistance furnace via a carbothermal reduction process. The experiment setup is similar to Ref. [22]. Briefly, 0.5 g of ZnO and graphite powder (well mixed by grinding) were loaded in the close end of one-end sealed slender quartz tube. Several p-type Si (1 0 0) (8–13 Ω cm) substrates coated with *c*-axis oriented ZnO seed layers sputtered by pulsed laser deposition (PLD) [23] were placed in the downstream of the source. The slender quartz tube was inserted into the large quartz tube with the source positioned in the center of the furnace. Then, the furnace was heated to 880 °C and kept for 30 min under air flow with a fixed flow rate of 2 sccm. The quartz chamber was evacuated to about 1 Torr during the whole synthesis process. After the reaction completed, uniform wax-like products were deposited onto all the seed wafers. Samples S1, S2 and S3 were obtained at 5, 10 and 15 cm away from the source materials.

The as-grown wax-like products were characterized by field emission scanning electron microscopy (FE-SEM) (FEI Sirion-200), X-ray diffraction (XRD) (Philips X'pert PRO diffractometer), and high-resolution transmission electron microscopy (HRTEM) (JEOL 2010). Raman spectrum was performed on a LabRamHR Raman Microspectroscope by using an Ar^+ laser excitation at 514.5 nm. FE properties were measured with diode configuration in a vacuum chamber at a pressure of about

* Corresponding author at: Anhui Institute of Optics and Fine Mechanics, Chinese Academy of Sciences, Hefei 230031, China. Tel.: +86 551 5593508; fax: +86 551 5593527.
E-mail address: xdfang@aiofm.ac.cn (X. Fang).

0925-8388/$ – see front matter © 2009 Elsevier B.V. All rights reserved.
doi:10.1016/j.jallcom.2009.11.038

10^{-5} Pa at room temperature. A dc voltage sweeping from 0 to 1500 V was applied to the nanowire arrays. The gap between the anode and ZnO sample was 1000 μm.

3. Results and discussion

For a given material, it has been demonstrated that the geometries of the 1-D emitters, including their aspect ratio, alignment degree and density, play an important role in FE performances [24]. Fig. 1 reveals the morphologies of the as-synthesized ZnO nanowire arrays. The FE-SEM cross sectional views of S1, S2 and S3 are shown in Fig. 1(a), (d) and (g), respectively. It can be clearly seen that ZnO nanowire arrays with uniform length grown perpendicularly to the Si wafers. The length of S1, S2 and S3 are 30.0 ± 1.7 μm, 46.2 ± 3.5 μm and 75.8 ± 1.7 μm, respectively. Ultra-

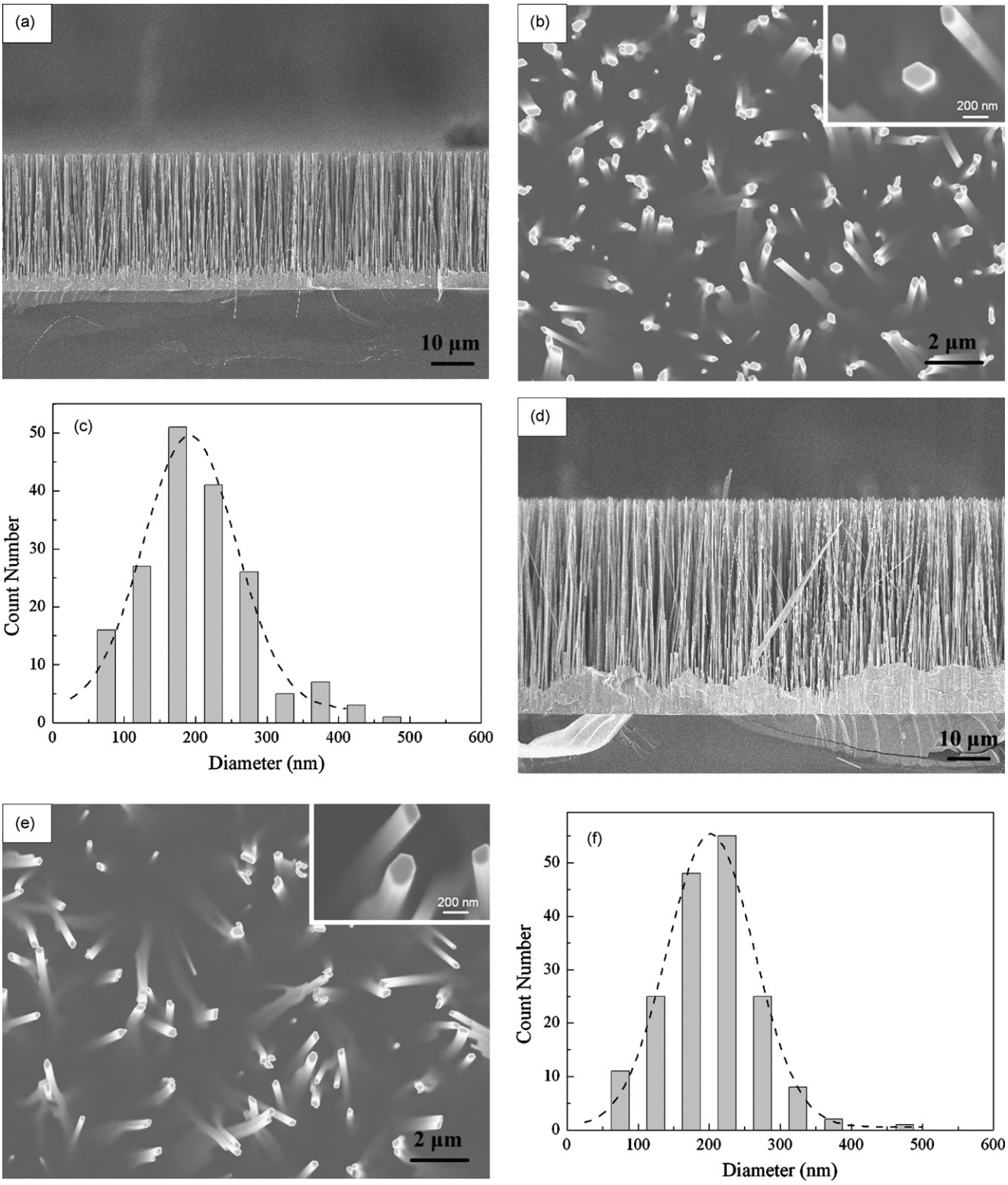

Fig. 1. FE-SEM images of as-synthesized ZnO nanowire arrays field emitters: (a), (d) and (g) are cross sectional views of samples S1, S2, and S3, respectively. (b), (e) and (h) are FE-SEM top views of samples S1, S2, and S3, respectively. The insets show enlarged views. (c), (f) and (i) are diameter histograms of S1, S2, and S3, respectively.

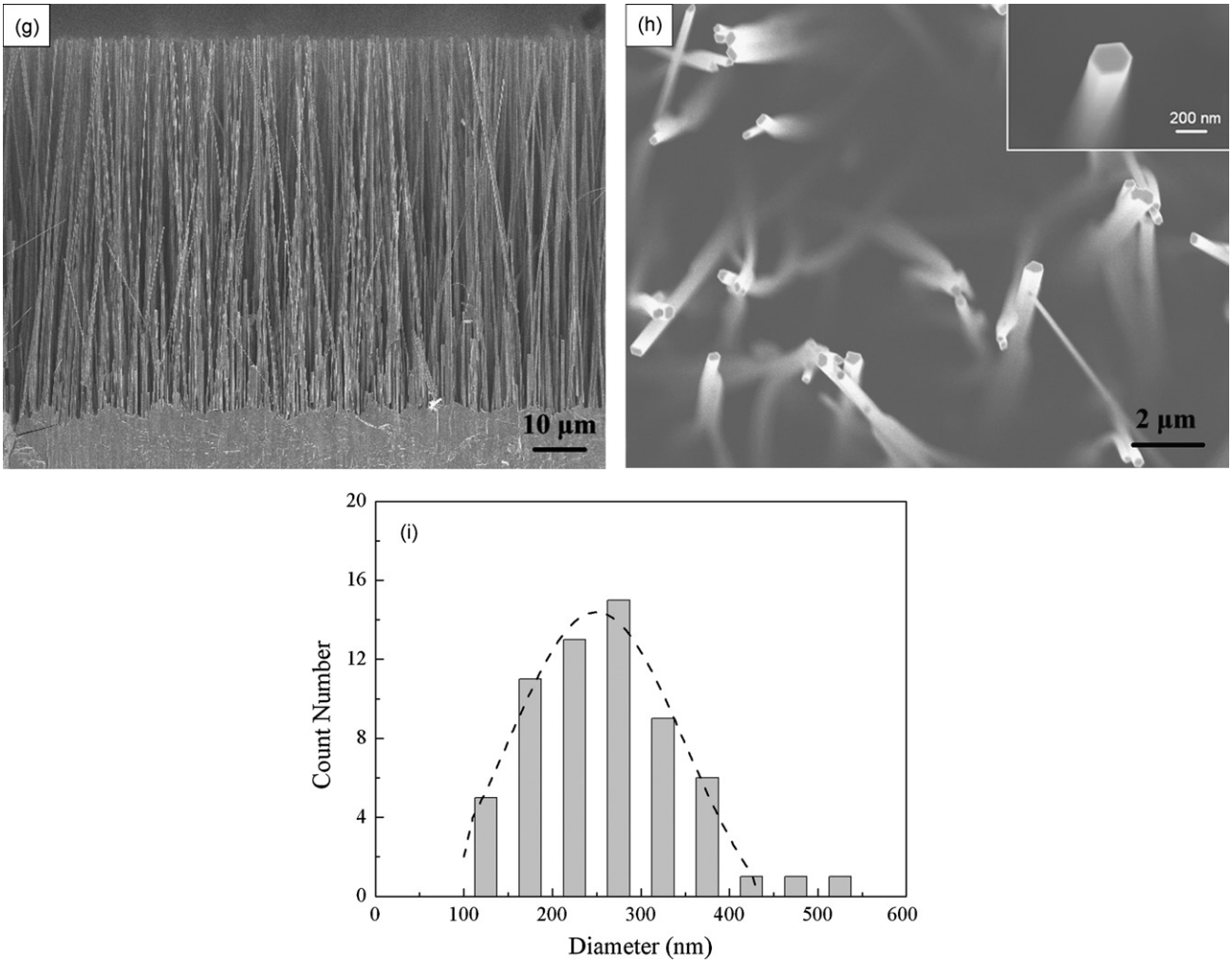

Fig. 1. (*Continued*).

long nanowires can be synthesized, possibly due to ample supply of Zn vapor (produced by carbothermal reduction of ZnO) and O_2 vapor (supplied by carrier gas) that facilitate fast growth of nanowire arrays. S3 is the longest, but S3 bent more than S1 and S2. The FE-SEM top views of samples S1, S2 and S3 (shown in Fig. 1(b), (e) and (h), respectively) demonstrate nanowires as well as nanowire bundles are grown almost vertically on the substrate. Some of nanowires are tilted and clung to each other at the tip area, which is attributed to electrostatic interaction of polar (0 0 0 1) faces [25] and flexibility of 1-D nanowires. S3 is seriously tilted at the top in comparison with S1 and S2, which is consistent with SEM cross sectional observations. SEM enlarged images in the inset of Fig. 1(b), (e) and (h) indicate the nanowires have flat quasi-hexagonal tops. The majority of nanowires have a diameter of about 200 nm, and some thin nanowires (<100 nm) can be observed. A few nanowires are thicker than 300 nm due to combination of several thin nanowires. Diameter histograms are shown in Fig. 1(c), (f) and (i), respectively. The mean diameter of S1, S2 and S3 can be estimated to 191 ± 130 nm, 202 ± 122 nm and 249 ± 150 nm, respectively by Gauss fitting of these histograms.

Fig. 2(a) shows a typical XRD pattern of the as-synthesized nanowire arrays. The sharp and dominant (0 0 2) diffraction peak

Table 1
Key parameters of typical 1-D ZnO emitters previously reported in the literature. The turn-on (V_{to}) and threshold (V_{th}) fields are defined as the field required at a current density of 1 μA/cm^2 and 1 mA/cm^2 [21], respectively. Turn-on field is also defined as the field required at a density of 0.01, 0.1 or 10 μA/cm^2, which are noted in bracket, β is the field enhancement factor.

Routes for improving FE performance	Morphology	V_{to} (V/μm)	V_{th} (V/μm)	β	Year	Reference
'Intrinsic' 1-D	Nanowires	6 (0.1)	11	847	2002	[11]
Emitters	Nanowires	18 (0.01)	24 (0.1)	372	2003	[7]
Doping & decorate & coupling	Al:ZnO nanowires	2.9	3.7	1710	2006	[14]
	Ag/ZnO nanorods	1.9 (10)	–	–	2007	[15]
	ZnO nanowires/C	<0.7	0.7	40,000	2004	[16]
Minimizing the radius of emission tips	Nanocones	3.7 (10)	–	2600	2007	[15]
	Nauopencils	0.85 (0.1)	5	8328	2007	[17]
	Tip fabrication	1.7 (10)	–	3513	2009	[18]
	Nanoneedles	2.4	6.5	1464	2005	[19]
	Nanopencils	3.8 (10)	5.8	2776	2009	[20]

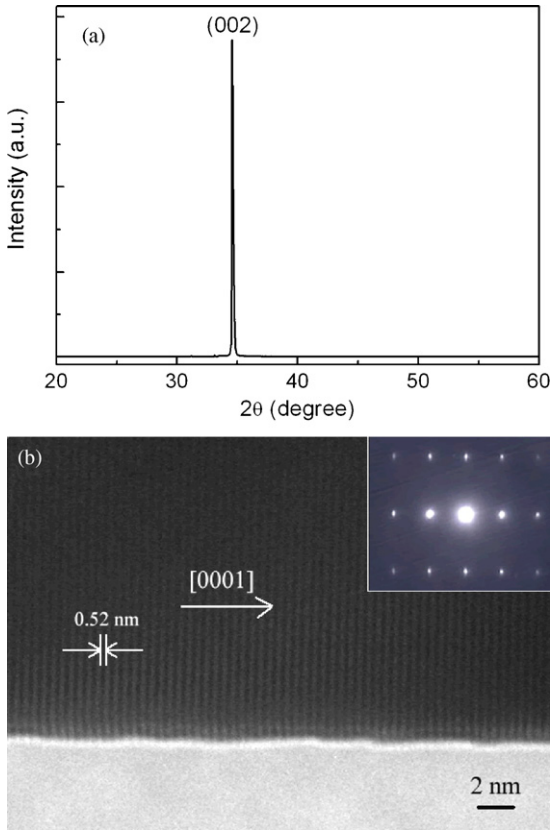

Fig. 2. Structural characterizations of ZnO nanowire arrays: (a) a typical XRD pattern; (b) HRTEM image of a single nanowire. The inset is the corresponding SAED pattern.

indicates the nanowire arrays are highly oriented with [0 0 2] direction normal to the substrate. The selected area electron diffraction (SAED) pattern in the inset of Fig. 2(b) can be indexed as single crystalline hexagonal wurtzite ZnO structure. A typical HRTEM image (Fig. 2(b)) also confirms the ZnO nanowire is well crystallized without any defects. The interplanar spacing of 0.52 nm corresponds to (0 0 2) planes of ZnO, indicating the growth direction is along *c*-axis, which agrees well with XRD result.

The Raman scattering was performed to investigate the vibrational property of the ZnO nanowires arrays. The micro-Raman peaks located at 439, 520, 580, and 1145 cm^{-1} were clearly observed in Fig. 3. All the scattering peaks except for 520 cm^{-1} (belonging to Si–Si scattering) can be well indexed to pure 1-D ZnO arrays [26,27]. The dominant peak at 439 cm^{-1} is attributed to ZnO non-polar optical phonons high E_2 mode. The relatively wide bands at 580 and 1145 cm^{-1} are of E_1 symmetry with LO and 2LO modes, respectively.

FE measurements of as-synthesized nanowire arrays were carried out in a vacuum chamber with a diode configuration, in which electrons would tunnel through a surface potential barrier and emit into a vacuum region at the presence of a high electric field. This phenomenon is seriously dependent on both the property of the emitter (work function φ) and the shape of the cathode [24]. And the relationship between emission current density and applied field can be described by Fowler–Nordheim (F–N) equation:

$$J = \frac{A\beta^2 E^2}{\phi} \cdot \exp\left(-\frac{B\phi^{3/2}}{\beta E}\right)$$

where J is the FE current density in the unit of A/cm^2, E is the applied electric field in the unit of V/μm, A and B are constants with values of 1.54×10^{-6} A V^{-2} eV and 6.83×10^3 V $eV^{-3/2}$ μm^{-1}, respectively. β

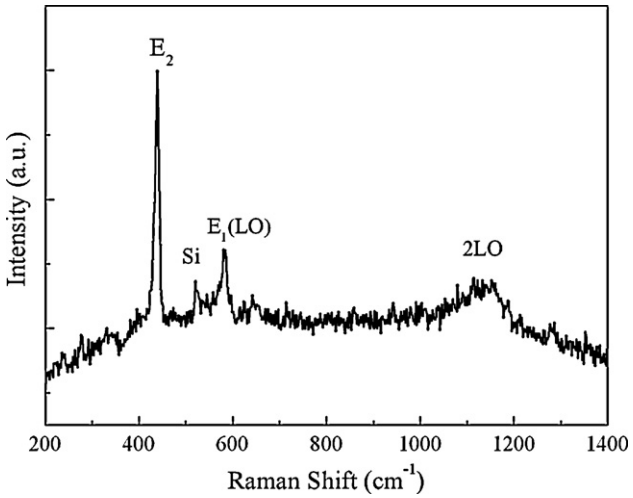

Fig. 3. Typical Raman spectrum of as-synthesized ZnO nanowire arrays.

is the geometric field enhancement factor, which reflects the ability of the emitters to enhance the local electric field.

The FE characteristics of ultra-long ZnO nanowire arrays emitters are shown in Fig. 4. The turn-on (V_{to}) fields (indicated by a dash horizontal line in Fig. 3) are 1.56, 1.27 and 1.08 V/μm for S1, S2 and S3, respectively. These values are much lower than the intrinsic nanowires emitters (not so long, with flat top) [7,11], and are comparable with those nanoneedles or nanopencils emitters with extreme sharp tips (<10 nm) [15,17]. However, controlled synthesis of ultra-long ZnO nanowire arrays is relatively easier than those nanoneedles emitters. Moreover, the thick nanowire arrays emitters with a diameter of ~200 nm and flat top should be more chemically stable than those sharp tips emitters due to much smaller quantities of dangling bonds, terraces and kinks exit.

FE characteristics were further demonstrated in the F–N plots shown in Fig. 5. The linear relationship between $\ln(J/E^2)$ and $1/E$ is given by the following equation:

$$\ln\left(\frac{J}{E^2}\right) = -\frac{B\phi^{3/2}}{\beta} \cdot \frac{1}{E} + \ln\left(\frac{A\beta^2}{\phi}\right)$$

And the F–N plots show roughly linearity for all the samples, implying that a quantum tunneling mechanism is responsible for the emission [3,13]. B is constant, taking the work function of ZnO as

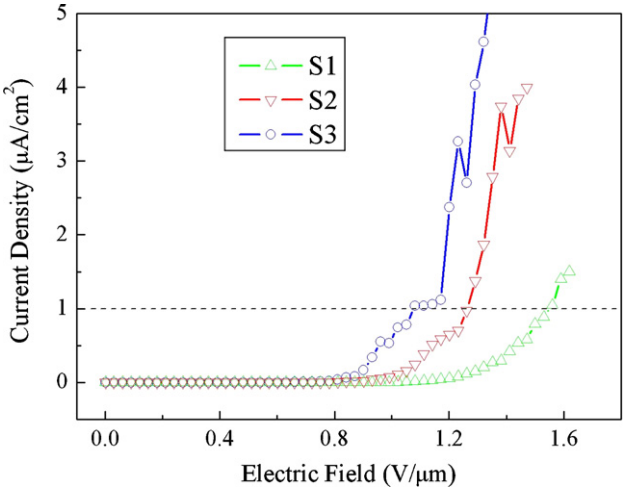

Fig. 4. *J*–*E* plots of ZnO nanowire arrays emitters. The dash line corresponds to the turn-on field.

Table 2
Summary of the dimensions of ZnO nanowire arrays emitters, turn-on voltage V_{to} and enhancement factor β.

Sample ID	Length (μm)	Diameter (nm)	Aspect ratio	Density (10^7/cm^2)	V_{to} (V/μm)	β
S1	30.0 ± 1.7	191 ± 130	~157	~8.1	1.56	7328
S2	46.2 ± 3.5	202 ± 122	~229	~4.0	1.27	9567
S3	75.8 ± 1.7	249 ± 150	~304	~1.3	1.08	9884

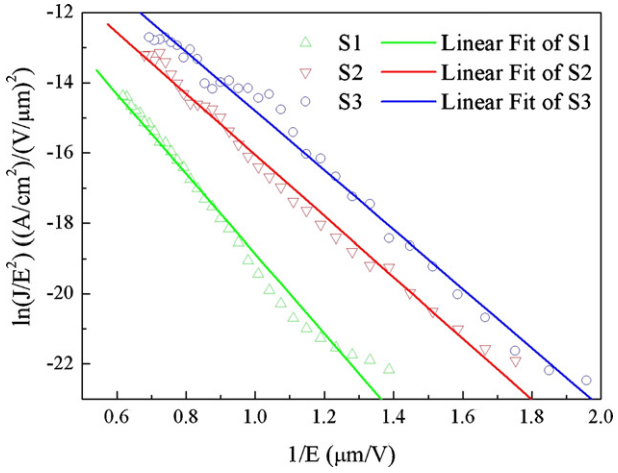

Fig. 5. F–N plots of ZnO nanowire arrays emitters.

5.3 eV [28], by calculation the slopes of fitting lines $k = -B\phi^{3/2}/\beta$ in Fig. 4, the values of β are estimated to be 7328, 9567 and 9884 for S1, S2 and S3, respectively. The calculated field enhancement factor β for ultra-long nanowire arrays is much higher than the previous reported values of 1-D ZnO arrays with sharp tips [18–20]. We conclude that such high enhancement factor is responsible for the low turn-on field of our sample.

The diameter, aspect ratio and density of nanowire arrays, as listed in Table 2, are critical factors to achieve high emission efficiency and field enhancement factor [5]. It can be clearly seen that the turn-on field decreases gradually with increasing the length of nanowire arrays (aspect ratio), and the field enhancement factor increases accordingly. In addition to aspect ratio, the areal density of the emitters should be taken into account. Low areal density with small number of emitting tips was generally considered as the reason for low emitting ability. While on the contrary, high areal density would result in screening effect and high turn-on field [29,30]. The effect of nanowires' density on the FE performances of 1-D ZnO emitter has been systematically investigated by Wang and Weintraub et al. The optimal areal density was assumed to be 6.4×10^9 and 7×10^8/cm^2, respectively [31,32]. The areal density of our emitters (~10^7/cm^2) is much lower than the optimized value. Therefore, the screen effect in our samples should be quite weak and the excellent FE performances were mainly attributed to high aspect ratio. Aligned ultra-long ZnO nanobelts (about 3.3 mm) have been synthesized by Ren' group via a molten-salted-thermal evaporation method, low turn-on field of 1.3 V/μm at a current density of 10 μA/cm^2 was achieved [33]. All these results indicate that increasing the aspect ratio by elongating the length of ZnO nanowires is an effective route to improve the FE performances of emitters.

4. Conclusions

In conclusion, we have successfully fabricated ultra-long ZnO nanowire arrays via a facile vapor phase transport process. The improved FE performances could be achieved by increasing the aspect ratio of 1-D ZnO arrays. Instead of commonly minimizing the tip radius of 1-D arrays, we adopted an alternative approach by increasing the length of 1-D arrays to increase the aspect ratio. FE characterization indicates that the turn-on field decreases with the length elongating of nanowire arrays, and ultra-low turn-on field about 1.08 V/μm were also achieved by this method, our results imply longer ZnO nanowire arrays are good candidate for field emitters in the future.

Acknowledgements

This work was supported by National Natural Science Foundation of China (No. 50672097) and Anhui Provincial Key Laboratory of Photonic Devices and Materials.

References

[1] J.M. Bonard, T. Stockli, O. Noury, A. Chatelain, Appl. Phys. Lett. 78 (2001) 2775.
[2] R.G. Forbes, J. Appl. Phys. 105 (2009) 114313.
[3] L.A. Ma, Y. Ye, L.Q. Hu, K.L. Zheng, T.L. Guo, Physica E 40 (2008) 3127.
[4] S.H. Luo, Q. Wan, W.L. Liu, M. Zhang, Z.F. Di, S.Y. Wang, Z.T. Song, C.L. Lin, J.Y. Dai, Nanotechnology 15 (2004) 1424.
[5] Z.H. Chen, Y.B. Tang, Y. Liu, G.D. Yuan, W.F. Zhang, J.A. Zapien, I. Bello, W.J. Zhang, C.S. Lee, S.T. Lee, J. Appl. Phys. 106 (2009) 064303.
[6] W.A. de Heer, A. Châtelain, D. Ugarte, Science 270 (1995) 1179.
[7] Y.K. Tseng, C.J. Huang, H.M. Cheng, I.N. Lin, K.S. Liu, I.C. Chen, Adv. Funct. Mater. 13 (2003) 811.
[8] J.U. Seo, S. Hasegawa, H. Asahi, J. Cryst. Growth 311 (2009) 2977.
[9] X.S. Fang, U.K. Gautam, Y. Bando, B. Dierre, T. Sekiguchi, D. Golberg, J. Phys. Chem. C 112 (2008) 4735.
[10] Y.B. Tang, H.T. Cong, H.M. Cheng, Appl. Phys. Lett. 89 (2006) 253112.
[11] C.J. Lee, T.J. Lee, S.C. Lyu, Y. Zhang, H. Rhu, H.J. Lee, Appl. Phys. Lett. 81 (2002) 3648.
[12] S.H. Jo, J.Y. Lao, Z.F. Ren, R.A. Farrer, T. Baldacchini, J.T. Fourkas, Appl. Phys. Lett. 83 (2003) 4821.
[13] J.B. You, X.W. Zhang, P.F. Cai, J.J. Dong, Y. Gao, Z.G. Yin, N.F. Chen, R.Z. Wang, H. Yan, Appl. Phys. Lett. 94 (2009) 262105.
[14] X.Y. Xue, L.M. Li, H.C. Yu, Y.G. Chen, Y.G. Wang, T.H. Wang, Appl. Phys. Lett. 89 (2006) 043118.
[15] C.H. Ye, Y. Bando, X.S. Fang, G.Z. Shen, D. Golberg, J. Phys. Chem. C 111 (2007) 12673.
[16] D. Banerjee, S.H. Jo, Z.F. Ren, Adv. Mater. 16 (2004) 2028.
[17] C.J. Park, D.K. Choi, J. Yoo, G.C. Yi, C.J. Lee, Appl. Phys. Lett. 90 (2007) 083107.
[18] I.C. Yao, P. Lin, T.Y. Tseng, Nanotechnology 20 (2009) 125202.
[19] Q. Zhao, H.Z. Zhang, Y.W. Zhu, S.Q. Feng, X.C. Sun, J. Xu, D.P. Yu, Appl. Phys. Lett. 86 (2005) 203115.
[20] J. Xiao, Y. Wu, W. Zhang, X. Bai, L.G. Yu, S.Q. Li, G.M. Zhang, Appl. Surf. Sci. 254 (2008) 5426.
[21] L.M. Li, Z.F. Du, C.C. Li, J. Zhang, T.H. Wang, Nanotechnology 18 (2007) 355606.
[22] C. Li, G.J. Fang, Q. Fu, F.H. Su, G.H. Li, X.G. Wu, X.Z. Zhao, J. Cryst. Growth 292 (2006) 19.
[23] W.W. Dong, X.B. Zhu, R.H. Tao, X.D. Fang, J. Mater. Sci.: Mater. Electron. 19 (2008) 538.
[24] X.S. Fang, Y. Bando, U.K. Gautam, C.H. Ye, D. Golberg, J. Mater. Chem. 18 (2008) 509.
[25] J.Z. Liu, S. Lee, K. Lee, Y.H. Ahn, J.Y. Park, K.H. Koh, Nanotechnology 19 (2008) 185607.
[26] H.M. Cheng, H.C. Hsu, Y.K. Tseng, L.J. Lin, W.F. Hsieh, J. Phys. Chem. B109 (2005) 8749.
[27] L. Liao, W.F. Zhang, H.B. Lu, J.C. Li, D.F. Wang, C. Liu, D.J. Fu, Nanotechnology 18 (2007) 225703.
[28] R.T.R. Kumar, E. McGlynn, C. McLoughlin, S. Chakrabarti, R.C. Smith, J.D. Carey, J.P. Mosnier, M.O. Henry, Nanotechnology 18 (2007) 215704.
[29] L. Nilsson, O. Groening, C. Emmenegger, O. Kuettel, E. Schaller, L. Schlapbach, H. Kind, J.M. Bonard, K. Kern, Appl. Phys. Lett. 76 (2000) 2071.
[30] X.M. Qian, H.B. Liu, Y.B. Guo, Y.L. Song, Y.L. Li, Nanoscale Res. Lett. 3 (2008) 303.
[31] X.D. Wang, J. Zhou, C.S. Lao, J.H. Song, N.S. Xu, Z.L. Wang, Adv. Mater. 19 (2007) 1627.
[32] B. Weintraub, S. Chang, S. Singamaneni, W.H. Han, Y.J. Choi, J. Bae, M. Kirkham, V.V. Tsukruk, Y.L. Deng, Nanotechnology 19 (2008) 435302.
[33] W.Z. Wang, B.Q. Zeng, J. Yang, B. Poudel, J.Y. Huang, M.J. Naughton, Z.F. Ren, Adv. Mater. 18 (2006) 3275.